ELSEVIER

Journal of Alloys and Compounds 330–332 (2002) 296–300

Journal of ALLOYS AND COMPOUNDS

www.elsevier.com/locate/jallcom

Raman spectroscopy studies on M_2RuH_6 where M=Ca, Sr and Eu

Hans Hagemann[a,*], Ralph O. Moyer[b]

[a]*Department of Chimie Physique, University de Genève, Geneva, Switzerland*
[b]*Department of Chemistry, Trinity College, Hartford, CT 06106-3100, USA*

Abstract

Characterization of ternary and quaternary metal hydrides by Raman spectroscopy appears to be rather scarce due primarily to the decomposition of the metal hydrides by the energy of the laser excitation source. We report the results of some recent room temperature Raman measurements collected with a 2–10 mW 488 nm laser source for M_2RuH_6 where M=Ca, Sr and Eu. The assignments from this study are combined with existing vibrational data for other metal hydrides.

Keywords: Transition metal compounds; Ternary metal hydrides; Raman spectroscopy

1. Introduction

Vibrational spectroscopic characterization of homoleptic ternary metal hydrides (TMHs) has been confined mostly to the K_2PtCl_6 structural type, and most of these data have been generated in the infrared (IR) region. These hydrido complexes possess O_h symmetry and are ideal to study because of their high metal–hydrogen structural and metal electronic symmetries. Kritikos and Noréus reported infrared (IR) spectroscopic data for several $[MH_6]^{4-}$ hydrides where M=Ru and Os [1]. Parker et al. characterized $Mg_2FeH_6(D_6)$ by inelastic neutron scattering, IR, and Raman techniques [2]. IR characterization of the mixed crystal system $[Ca_{2-x}Eu_x]RuH_6$ has been studied by Moyer et al. [3]. In general Raman techniques have been seen as a complementary spectroscopic tool to IR methods; but in the past have been difficult to apply to metal hydrides because of radiation induced compound decomposition. We wish to report the results of some successful Raman experiments for M_2RuH_6 where M=Ca, Sr, or Eu.

2. Experimental

The formation of the TMHs has been reported elsewhere [4,5]. Briefly it consists of three steps: (1) the high temperature vacuum purification of the alkaline earth metals or Eu, (2) the formation of the metal binary hydrides of these metals by direct combination of the elements and (3) the high temperature gas/solid-phase synthesis of the TMH by combining the binary hydride with the rarer platinum metal in an hydrogen (deuterium) atmosphere.

The samples were ground into very fine powders and portions of each were transferred into 1-mm glass capillary tubes to a height of approximately 4–5 cm.

The Raman spectra were collected with a Kaiser Holospec f/1.8 spectrograph equipped with a liquid nitrogen cooled CCD camera. The argon laser excitation source was powered at approximately 2–10 mW. The wavelength of the incident radiation was 488 nm. All spectra were obtained at room temperature and the scanning range was confined to 2000–600 cm^{-1}. Acquisition times ranged from 15 min to 1.5 h.

3. Results and discussion

M_2RuH_6 (M=Ca, Sr and Eu) adopt the well known K_2PtCl_6 structure, shown in Fig. 1. The structure can be viewed as cubic close packing of low spin six coordinate hexahydridoruthenate(II), i.e. $[RuH_6]^{4-}$, shown as purple octahedra with the divalent counter cations (Ca^{2+}, Sr^{2+} or Eu^{2+}) occupying all of the tetrahedral sites noted as blue spheres. Six normal vibrational modes are assigned to the O_h $[RuH_6]^{4-}$ units, i.e. two (IR) active, three Raman (R) active and one IR inactive [6]. The terms assigned to the three Ru–H/D vibrational stretches (υ) are A_{1g} (R), E_g (R)

*Corresponding author.
E-mail address: hans-rudolf.hagemann@chiphy.unige.ch (H. Hagemann).

0925-8388/02/$ – see front matter
PII: S0925-8388(01)01540-7

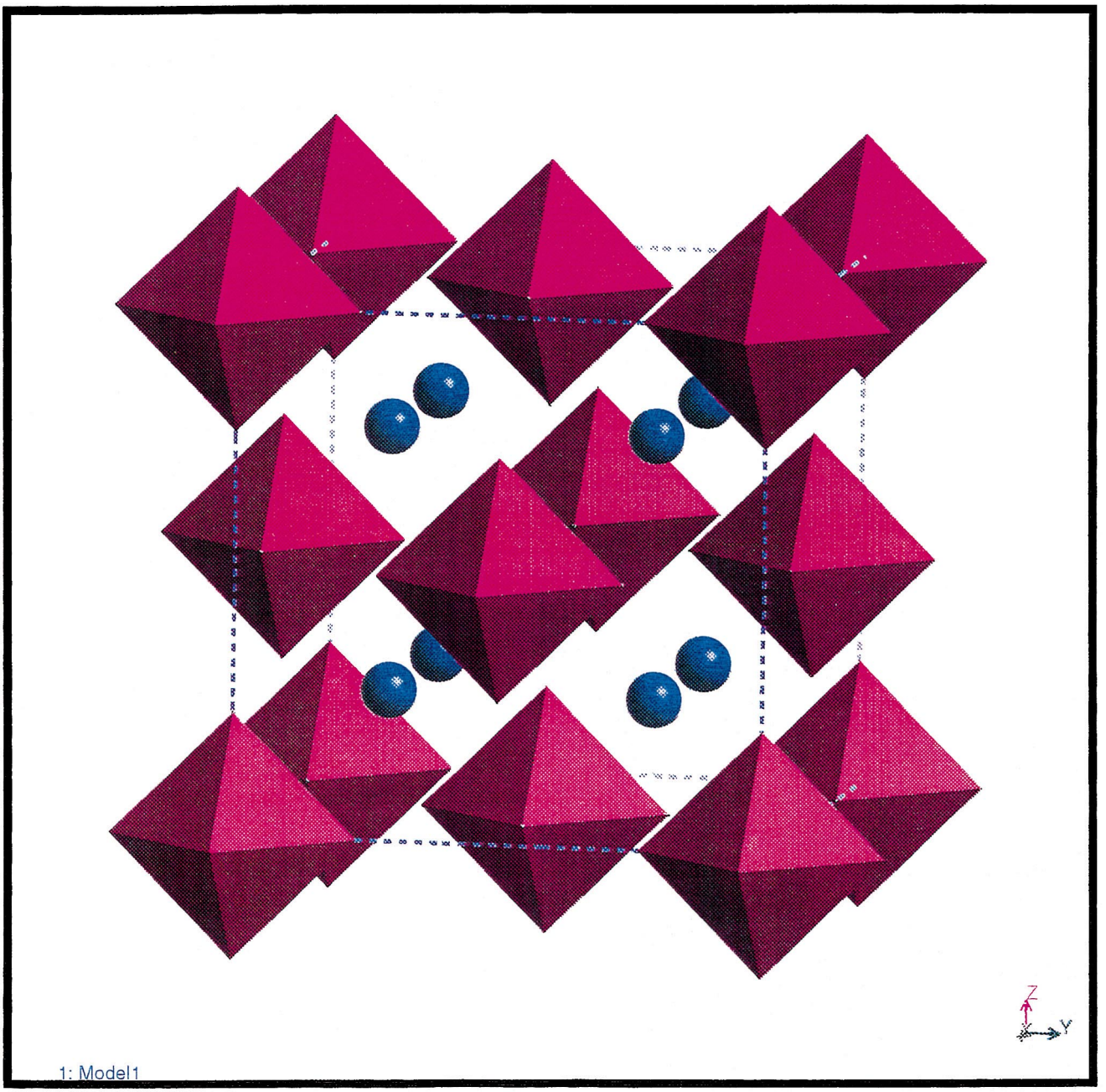

Fig. 1. M_2RuH_6 crystal structure where M=Ca, Sr or Eu.

and T_{1u} (IR). Those terms for the three Ru–H/D bending modes (σ) are T_{2g} (R), T_{1u} (IR) and T_{2u} (IR and Raman silent).

Raman spectra for Ca_2RuH_6, Ca_2RuD_6, Sr_2RuH_6 and Eu_2RuH_6 are shown in Fig. 2. The Raman peaks along with their respective assignments are given in Table 1. The comparison of the Raman spectra of Ca_2RuH_6 and Ca_2RuD_6 shows the expected isotope effect, i.e. $\nu_H/\nu_D=1.4$. Raman data for Mg_2FeH_6 and Mg_2FeD_6 are included for purposes of comparison [2].

It has been reported that Raman intensities for XY_6 units normally follow the order $A_{1g}>E_g>T_{2g}$ [7]. For the Mg containing hydrides, the Eg mode appears to be accidently at the same frequency as the A_{1g} mode [2]. Fig. 2 shows that for the samples studied in this work the T_{2g} mode has much stronger Raman intensity than the A_{1g} and E_g modes. It is possible that the resonant Raman contributions yield these intensity changes. However, in the absence of Raman spectra using other excitation wavelengths any further explanation remains too speculative.

The Raman intensities for the brick red compound Eu_2RuH_6 are much weaker than those of the other samples which are gray. These intensity reductions may be caused by the absorption of the blue laser light by this sample.

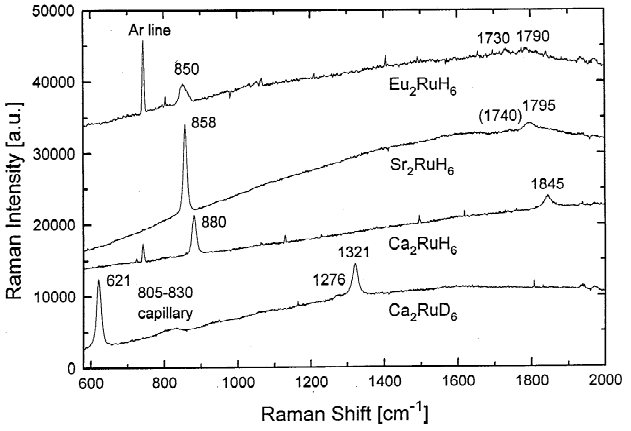

Fig. 2. Raman spectra of M_2RuH_6 where M = Ca, Sr, Eu.

Table 1

Ternary hydride	Raman vibrational data (cm^{-1})[a]			$\upsilon_{A1g}/\upsilon_{T2g}$
	M–H/D (stretching)		M–H/D (bending)	
	A_{1g}	E_g	T_{2g}	
Ca_2RuH_6	1845(m)		880(s)	2.1
Ca_2RuD_6	1321(m)	1276(vw)	621(s)	2.1
Sr_2RuH_6	1795(w)	1740(vvw)	858(s)	2.1
Eu_2RuH_6	1790(vw)	1730(vvw)	850(m)	2.1
Mg_2FeH_6 [2]	1873(s)	1873	1019 and 1057(vw)	1.8
Mg_2FeD_6 [2]	1342(s)	1342	730(w)	1.8

[a] v, very; s, strong; m, medium; w, weak.

The ratios of the stretching to bending frequencies for the Raman $\upsilon(A_{1g})/\upsilon(T_{2g})$ for the Ru containing ternary compounds are constant at 2.1. The corresponding ratios for Mg_2FeH_6 is 1.8.

It has been noted by others that there is an inverse relationship between the IR active stretching vibrational mode (T_{1u}) and the unit cell length (a) [1,3]. This trend is noted as well in the Raman spectra (see Table 2).

Attempts have been made to apply equations which express the decreasing changes in the asymmetric IR Ru–H stretching frequencies with increasing changes in the unit cell size. For example, a nonlinear equation has been used to express these changes over a range of a values from 6.656 to 8.0238 Å for several Ru containing TMHs and a linear equation has been shown to describe similar changes in the Ru containing mixed crystal TMH $[Ca_{2-x}Eu_x]RuH_6$ system with a much shorter range of 7.227–7.566 Å [3].

Table 2
Vibrational data-M_2RuH_6

Compound	a (Å)	Infrared (cm^{-1}) T_{1u}	Raman (cm^{-1})	
			A_{1g}	T_{2g}
Ca_2RuH_6	7.227	1564	1845	880
Sr_2RuH_6	7.609	1482	1795	858
Eu_2RuH_6	7.566	1480	1790	850

Table 3
Experimental and interpolated Ru–H bond lengths

Compound	$0.25\times a$ (Å)	d(Ru–D) Å Neutron data [1,4,9][a]	$\nu(T_{1u})^{-2/3}\times 10^3$ $(cm^{-1})^{-2/3}$
Mg_2RuH_6	1.664	1.673(4)	6.784
Ca_2RuH_6	1.808	[1.675]	7.404
Sr_2RuH_6	1.902	1.69(1)	7.674
Ba_2RuH_6	2.007	1.73(1)	7.838
Yb_2RuH_6	1.812	[1.675]	7.448
Eu_2RuH_6	1.892	[1.69]	7.681

[a] [ ], Predicted values.

Ideally there should be a relation between the equilibrium internuclear distances (r_{eq}) and the bond force constant (F_{eq}). Badger proposed a rule to account for the systematic variation in the vibrational frequency with changes in the bond distances for a number of systems, one of which being the polyatomic octahedral SF_6 [8]. He noted that the cubic root of the force constant was directly related to the equilibrium bond distance

$$[F_{eq}]^{-1/3} = A(r_{eq}) - B \quad (1)$$

As the force constant is proportional to the square of the vibrational frequency Eq. (1) can be rewritten as expression (2)

$$[\nu(T_{1u})]^{-2/3} = \alpha(r_{eq}) - \beta \quad (2)$$

X-ray diffraction structural analysis provides only an estimate of the internuclear metal–hydrogen bond distance, i.e. $0.25\times a$. A complete structural analysis by neutron diffraction techniques allows for an accurate determination of the Ru–H bond distances. The available Ru–D data are collected in Table 3 [1,4,9].

Fig. 3 plots the value of $[\nu(T_{1u})]^{-2/3}$ vs. the available Ru–D bond lengths for Mg_2RuD_6, Sr_2RuD_6, and Ba_2RuD_6. The data points for M = Mg, Sr and Ba are

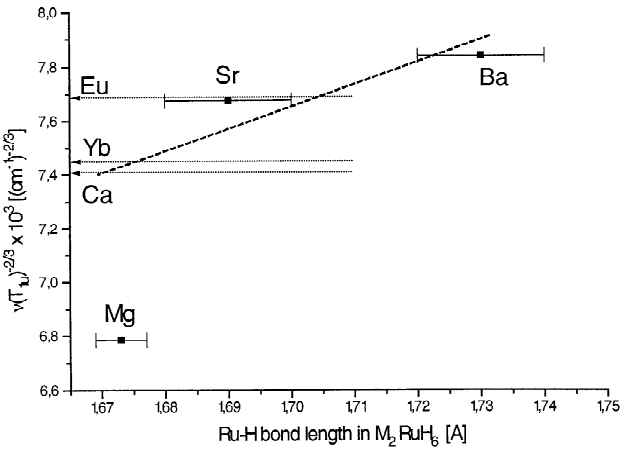

Fig. 3. Badger's rule — applied to the T_{1u} stretching mode in M_2RuH_6 where M = Mg, Ca, Yb, Sr, Eu and Ba.

shown with their standard deviations of the Ru–D bond lengths as obtained from neutron diffraction. In spite of the relatively large experimental error of the Ru–D bonds, it appears clearly that there is no linear relation connecting the three data points.

The values of $\nu(T_{1u})^{-2/3}$ for M=Ca, Yb and Eu are indicated by the dotted lines in Fig. 3. From crystal chemical considerations, one expects that the Ru–D bond lengths in Ca_2RuD_6 and Yb_2RuD_6 lie between the values found for the Mg and Sr compounds (1.673 and 1.69 Å, respectively). The bond length for Eu_2RuD_6 is expected to be very similar to that found in Sr_2RuD_6 as the ionic radii of Sr^{2+} and Eu^{2+} are very close.

Mg_2RuH_6 is unique in the sense that the Ru–H bond distances is very close to $0.25\times a$; while this is not the case for the other TMHs. In addition, the observed Ru–H stretching frequency is significantly higher for this compound when compared to the other ruthenium containing TMHs. As a general rule for inorganic molecular ions, e.g. SO_4^{2-}, the vibrational stretching frequencies should not change by more than a couple of percent depending on the counterion [10].

In this case we observed a 15% change in going from Mg_2RuH_6 to Ca_2RuH_6 which suggests to us the presence of an unspecified vibrational coupling in the Mg_2RuH_6 crystal lattice.

If Badger's rule holds for at least a part of the ternary ruthenium hydrides studies here, it seems therefore more likely to connect the data points of the Sr and Ba compounds rather than those of the Sr and the somewhat compressed Mg compounds. This is attempted with the dashed line in Fig. 3 with the additional constraint to intersect the values $\nu(T_{1u})^{-2/3}$ for M=Ca and Yb at a Ru–H bond length >1.673 Å. This construction leads to an estimated Ru–H bond lengths of ~1.675 Å for Ca_2RuH_6 and Yb_2RuH_6, a value much closer to the bond length in Mg_2RuH_6 than in Sr_2RuH_6. Further experiments will show whether Badger's rule may indeed be used to predict metal–hydrogen bond lengths in this class of compounds.

In summary, the existing (albeit limited) vibrational spectroscopic data for ternary metals hydrides are tabulated in Table 4. For those data where both IR and Raman data exist it is interesting to note that a much greater splitting between the IR and Raman active stretching modes for the Ru containing TMHs than for Mg_2FeH_6. In contrast, the IR and Raman active bending mode frequencies are closer for the Ru containing TMHs. The advent of newer Raman instrumentation now offers opportunities for more vibrational spectroscopic experiments to be undertaken not only to fill in the gaps in Table 4 but also to extend the technique to the many other structurally different ternary metal hydrides.

4. Conclusion

We have succeeded in obtaining room temperature Raman data for several ruthenium containing ternary metal hydrides using low power laser illumination and high sensitivity data collection. These new Raman data complement existing infrared data. All these vibrational spectra show systematic changes with changes in the crystal lattice dimensions. Badger's rule may possibly be used to predict the Ru–H bond lengths in the absence of neutron diffraction data. For example, in the present study, the Ru–H bond distance is estimated to be close to 1.675 for Ca_2RuH_6.

Table 4
Vibrational data — ternary metal hydrides

Compound	M–H(D) stretching modes			M–H(D) bending modes			Libr.
	A_{1g}(R)	E_g(R)	T_{1u}(IR)	T_{2g}(R)	T_{1u}(IR)	T_{2u}(IA)	T_{1g}(IA)
Mg_2FeH_6	1873	1873	1746	1019–57	899	836	460
Mg_2FeD_6	1342	1342	1260	730	661	599	324
Mg_2RuH_6			1783				
Mg_2RuD_6			1279				
Ca_2RuH_6	1845		1546	880	896		
Ca_2RuD_6	1321	1276	1128	621	646		
Sr_2RuH_6	1795	1740	1482	858	878		
Ba_2RuH_6			1438				
Ba_2RuD_6			1023				
Yb_2RuH_6			1550				
Eu_2RuH_6	1790	1730	1480	850	878		
Mg_2OsH_6			1849		864		
Mg_2OsD_6			1325				
Ca_2OsH_6			1637				
Sr_2OsD_6			1575				
Ba_2OsH_6			1505				
Ba_2OsD_6			1078				

Values from Refs. [1–3] and this work.

Acknowledgements

The Swiss National Science Foundation and a Trinity College Research Grant are gratefully acknowledged HH and by ROM Jr, respectively.

References

[1] M. Kritikos, D. Noréus, J. Solid State Chem. 93 (1991) 256.
[2] S.F. Parker, K.P.J. Williams, M. Bortz, K. Yvon, Inorg. Chem. 36 (1997) 5128.
[3] R.O. Moyer Jr., J.R. Wilkins, P. Ryan, J. Alloys Comp. 290 (1999) 103.
[4] R.O. Moyer Jr., C. Staniski, J. Tanaka, M.I. Kay, R. Kleinberg, J. Solid State Chem. 3 (1971) 541.
[5] J.S. Thompson, R. Lindsay, R.O. Moyer Jr., Inorg. Chem. 14 (1975) 1866.
[6] K. Nakamoto, in: 4th Edition, Infrared and Raman Spectra of Inorganic and Coordination Compounds, Vol. II–15, Wiley-Interscience, New York, 1986, p. 148.
[7] K. Nakamoto, in: 4th Edition, Infrared and Raman Spectra of Inorganic and Coordination Compounds, Vol. II–15, Wiley-Interscience, New York, 1986, p. 154.
[8] R.M. Badger, J. Chem. Phys. 1 (1935) 710.
[9] B. Huang, F. Bonhomme, P. Selvan, K. Yvon, P. Fischer, J. Less-Common Metals 171 (1991) 301.
[10] I.A. Degen, G.A. Newman, Spectrochim. Acta 49A (1993) 859.